Journal of Nuclear Materials 504 (2018) 101–108

Contents lists available at ScienceDirect

Journal of Nuclear Materials

journal homepage: www.elsevier.com/locate/jnucmat

Differential dpa calculations with SPECTRA-PKA

M.R. Gilbert [a, *], J.-Ch. Sublet [a, b]

[a] Culham Centre for Fusion Energy, United Kingdom Atomic Energy Authority, Culham Science Centre, Abingdon, OX14 3DB, UK
[b] Nuclear Data Section, International Atomic Energy Agency, P.O. Box 100, 1400, Vienna, Austria

HIGHLIGHTS

- SPECTRA-PKA processes nuclear reaction data on a per channel basis.
- Displacements per atom (dpa) rates are calculated for each reaction channel.
- Scattering reactions dominate fission damage, but less so in fusion.
- (n, 2n) reactions can be as important for damage as scattering.
- Transmuting reactions can also contribute non-negligibly to dpa rates.

ARTICLE INFO

Article history:
Received 23 February 2018
Received in revised form
14 March 2018
Accepted 16 March 2018
Available online 21 March 2018

Keywords:
Displacements per atom (dpa)
Nuclear data processing
Neutron irradiation
Nuclear reaction channels

ABSTRACT

The processing code SPECTRA-PKA produces energy spectra of primary atomic recoil events (or primary knock-on atoms, PKAs) for any material composition exposed to an irradiation spectrum. Such evaluations are vital inputs for simulations aimed at understanding the evolution of damage in irradiated material, which is generated in cascade displacement events initiated by PKAs. These PKA spectra present the full complexity of the input (to SPECTRA-PKA) nuclear data-library evaluations of recoil events. However, the commonly used displacements per atom (dpa) measure, which is an integral measure over all possible recoil events of the displacement damage dose, is still widely used and has many useful applications – as both a comparative and correlative quantity. This paper describes the methodology employed that allows the SPECTRA-PKA code to evaluate dpa rates using the energy-dependent recoil (PKA) cross section data used for the PKA distributions. This avoids the need for integral displacement kerma cross sections and also provides new insight into the relative importance of different reaction channels (and associated different daughter residual and emitted particles) to the total integrated dpa damage dose. Results are presented for Fe, Ni, W, and SS316. Fusion dpa rates are compared to those in fission, highlighting the increased contribution to damage creation in the former from high-energy threshold reactions.

1. Introduction

The displacement per atom (dpa) measure of damage dose due to particle bombardment (irradiation) of materials is commonly (ubiquitously) used to estimate the atomic-level structural damage in irradiated materials. The so-called Norgett-Robinson-Torrens dpa or NRT-dpa [1] has been the standard evaluation method for several decades. While such an integral measure has obvious limitations [2,3], and should be viewed as an "atomic damage dose" rather than a quantitative measure of damage creation [4], it has nonetheless shown to correlate with certain damage phenomena (see, for example [5]). Furthermore, it provides a useful standard comparison between different irradiation experiments reported in the literature (provided the dpa model remains unchanged), and so there is continued interest in stable calculation of NRT-dpa values. For neutron irradiation, dpa rates are often obtained by folding the energy-dependent irradiation spectrum, usually measured/evaluated in units of neutrons cm^{-2} s^{-1}, with (neutron) energy-dependent displacement kerma (kinetic energy released per unit mass) cross sections σ_d (expressed in eV barns units in this context, where 1 b is 10^{-24} cm^2). A modified Kinchin-Pease [6] formula, which has subsequently become known as the NRT model, is then applied to the scalar product result to obtain a dpa contribution from a particular target nuclide. A sum over all target nuclides in a

* Corresponding author.
E-mail address: mark.gilbert@ukaea.uk (M.R. Gilbert).

https://doi.org/10.1016/j.jnucmat.2018.03.032

material or element (weighted according to their fractional concentrations) produces the total NRT-dpa per second [4] for that composition.

However, the σ_d cross section vectors, which are essentially totals over all possible reactions on a given target nuclide, must be pre-computed from the raw nuclear reaction cross section data and are thus already integral values. In this paper we describe a different approach, wherein the dpa formulas can be applied separately for each nuclear reaction based on the energy spectrum of the reaction daughter products (the primary knock-on atoms or PKAs). The resulting dpa rates associated with each nuclear reaction can still be summed to recover the full dpa rate in a material, but the individual dpa contributions provide useful additional information and insights – for example, showing if neutron multiplication reactions contribute significantly to the total dpa rate. They also highlight the importance of the nuclear-reaction data for certain channels, which might otherwise have been neglected because they are not important for the nuclear fission criticality or burn-up calculations that are usually targeted when developing nuclear data libraries (although they may be relevant for transmutation and/or radioactivity).

The methodology implemented in the recently developed SPECTRA-PKA code [7], which is now freely available to download [8], is described below. Several examples are presented and discussed, including comparisons between nuclear fission and fusion environments.

2. Methodology

For a given nuclear reaction on a target (parent) nuclide the recoil energy distribution for the daughter (that might be a different nuclei to the parent) is readily available for neutron interactions (and other light charged particles, such as protons) from various alternative nuclear data libraries. For SPECTRA-PKA and its parent code – the inventory simulation system FISPACT-II [9] – the recommended libraries are from the TENDL [10,11] series (TENDL-2017 [12] is the latest release) because they are the most complete (for cross sections, angular recoil distributions and emitted spectra) and modern (they contain, for example, covariance data) databases available.

The processing code NJOY [13] is commonly used to evaluate the displacement kerma cross section (a derived quantity) for a given target nuclide from this primary input library data, which can then be combined with the incident (neutron) particle spectrum to calculate the dpa rate for that nuclide. NJOY applies the Lindhard-Scharff-Schiøtt (LSS) partition theory [14,15] to evaluate the damage energy available to cause displacements for the recoiling daughter nuclide (the PKA) j as a function of its energy (E_{PKA}). Focussing on neutron interactions (the evaluation method for other irradiating particles is similar), the subsequent sum across all E_{PKA} values for the daughter produced at each neutron energy E_n in eV is multiplied by the energy-dependent reaction cross section $\sigma(E_n)$ to give the contribution to the total displacement kerma cross section from that particular reaction. There is usually a probability distribution of PKA energies for each neutron energy due to the energy-angular dependence of multiple emitted particles produced in nuclear reactions.

The total displacement kerma cross section σ_i^{disp} for target nuclide i at neutron energy E_n is then the sum over all possible nuclear reactions $i \rightarrow j$ (denoted as ij):

$$\sigma_i^{disp}(E_n) = \sum_j \sigma_{ij}(E_n) \sum_k T_j\left(E_{PKA}^k\right) P_{ij}\left(E_{PKA}^k, E_n\right), \tag{1}$$

where $P_{ij}(E_{PKA}, E_n)$ is the probability of producing daughter PKA energy E_{PKA} for reaction $i \rightarrow j$ at neutron energy E_n. Each probability is multiplied by the damage energy T_j for daughter j as a function of PKA energy according to a modified version [15] of LSS partition theory [14]. The sum (or integral if a continuous distribution function is available) over the k possible PKA energies is sometimes referred to as the transferred energy for reaction $i \rightarrow j$ at the given neutron energy [4]. $\sigma_{ij}(E_n)$ is the cross section for reaction $i \rightarrow j$ at energy E_n.

An inventory code, such as FISPACT-II, applies the NRT formula to find the NRT-dpa cross section:

$$\sigma_i^{dpa}(E_n) = \frac{0.8\sigma_i^{disp}(E_n)}{2E_d}, \tag{2}$$

and then folds (i.e. vector dot or scalar product) the result with the neutron flux vector to give the dpa rate for each target in a material, which are then weighted by the inventory (nuclide) composition and summed to evaluate the total dpa rate in the material. E_d is known as the threshold displacement energy, and is the energy required to produce a Frenkel pair atomic defect in the material lattice.

SPECTRA-PKA [7], on the other hand, reads a data-library of vectors over k

$$\left\{\sigma_{ij}(E_n) P_{ij}\left(E_{PKA}^k, E_n\right)\right\} \equiv \left\{m_{kn}^{ij}\right\},$$

where m_{kn}^{ij} is the cross section in barns for a recoil in energy group (or bin) k for an incident neutron in energy group n for reaction $i \rightarrow j$ (following the same notation conventions used in Refs. [7,16]). These vectors, which are processed into a grid of energy bins by the GROUPR module of NJOY [13], are folded with the incident particle fluxes ϕ_n to calculate PKA distributions. However, they can also be used to evaluate the displacement kerma cross section for individual reactions by multiplying each m_{kn}^{ij} value by the damage energy $T_j^k (\equiv T_j(E_{PKA}^k))$ associated with the emitted daughter j at PKA energy k.

The damage energy is obtained via the formulas described by Robinson [17], assuming that the "target" atom for the collisions of the daughter projectile j from reaction $i \rightarrow j$ are the same as the original parent atom i (a valid approximation in most situations). From Ref. [17], we have

$$T_j^k \equiv T_j\left(E_{PKA}^k\right) = \frac{E_{PKA}^k}{\left(1 + k_{LSS}\, G\left(\frac{E_{PKA}^k}{E_{LSS}}\right)\right)}, \tag{3}$$

where E_{LSS} was introduced in Ref. [15] to make the description of nuclear stopping dimensionless and k_{LSS} is a parameter (constant for a given projectile-target pair) which collects together constants of the Thomas-Fermi description of atomic interactions [14]. For a projectile j with mass and atomic number M_j and Z_j, respectively, and target i with equivalent M_i and Z_i, these LSS parameters are defined via:

$$E_{LSS} = \frac{Z_j Z_i e^2}{a_{12}} \frac{1 + A}{A},$$

$$k_{LSS} = \frac{32}{3\pi} \left(\frac{m_e}{M_i}\right)^{1/2} \frac{(1 + A)^{3/2} Z_j^{2/3} Z_i^{1/2}}{\left(Z_j^{2/3} + Z_i^{2/3}\right)^{3/4}},$$

where m_e is the mass of an electron (=5.4857991E-4 atomic mass units u) and e^2 is the square of the elementary charge (=1.4399652 eV nm), and

$$A = M_i/M_j,\ a_{12} = \left(\frac{9\pi}{128}\right)^{1/3} \frac{r_{\text{bohr}}}{\left(Z_j^{2/3} + Z_i^{2/3}\right)^{1/2}}.$$

a_{12} is the screening length for ion-atom interactions using the Bohr radius r_{bohr} (=0.52917722 nm). $G(\varepsilon)$ is the universal function [1] and is evaluated via a numerical approximation [18]:

$$G(\varepsilon) = \varepsilon + 0.40244\varepsilon^{3/4} + 3.4008\varepsilon^{1/6}.$$

Note that this formalism is actually the Lindhard et al. [14,15] formalism for non-identical target and projectile atoms (described by Robinson [17]), rather than the equations for damage energy applied by Norgett-Robinson-Torrens in their original presentation of the modified Kinchin-Pease method for displacement dose rates [1], which was partially taken from an earlier work by Robinson [18]. That original approach in Ref. [1] only considered an expression for k_{LSS} appropriate to the case where the recoiling atom and target atoms are identical. The complete formalism shown here is more appropriate for SPECTRA-PKA where we may be considering reaction channels with a recoiling particle j that has a very different mass to that of the parent (and recoil target) i. For example, light atoms of helium and hydrogen are emitted from many threshold transmuting (different proton number Z of daughter) reactions. This somewhat overcomes the limitations noted in Ref. [1], that the formulation therein was strictly limited to monatomic systems.

However, the assumption that the target atom is the same as the original parent atom in a particular reaction channel still limits the validity. In most situations, including mono-elemental systems and alloys of similar mass metals, this approximation is reasonably valid because the PKA daughter atom will be moving through a lattice of similar mass (to the parent) atoms. In more heterogeneous material compositions with a wide distribution of atomic masses, such as in a heavy-metal oxide or a ceramic, an alternative approach should be applied: the concentrations of different atomic species can be taken into account when evaluating the displacements caused by a recoil of each species. For example, see Ref. [20], which also discusses the use of variable threshold displacement energies in the NRT formula.

Following the calculation of the damage energy via equation (3), the total NRT-dpa rate for the given $i \rightarrow j$ reaction channel is obtained via:

$$\text{dpa}_{ij}\ \text{rate} = \frac{0.8}{2E_d} \sum_n \phi_n \sum_k m_{kn}^{ij} T_j^k, \tag{4}$$

where ϕ_n is the particle (neutron) flux in units of neutrons $\text{cm}^{-2}\ \text{s}^{-1}$ at neutron energy E_n. In SPECTRA-PKA the particle fluxes and recoil cross sections are all defined on a grid of energy bins/groups (n or k bins, respectively, in equation (4)), and so the $\{T_j^k\}$ vectors are also calculated as a set of (k) bin boundaries. Subsequently, the T_j^k values used in equation (4) are the midpoint damage-energy of each bin.

The total dpa rate in a material can be recovered from equation (4) by summing over the j possible reactions (the result is equivalent to equations (1) and (2) rearranged), and then over the i different reaction targets in the system with a relative concentration weighting.

3. Example results

Fig. 1 demonstrates the application of the methodology described in the previous section. Fig. 1a shows the PKA spectra, calculated by SPECTRA-PKA, for pure ^{56}Fe (91.754% of pure iron) under the neutron irradiation conditions predicted in the first wall of a conceptual design of a demonstration fusion power plant [19]. The neutron irradiation spectrum for this scenario is also shown in the plot. The input nuclear data for these results, and for all results in the present work, are recoil cross section matrices produced by NJOY [13] from the raw, point-wise data form of the TENDL-2015 [21] library of nuclear reaction cross sections and energy-angular distributions. Fig. 1a shows, for example, the dominance of the contribution from elastic scattering, particularly at PKA energies below 100 keV. It also shows that non-scattering reaction channels, such as neutron multiplication (n, 2n) [one incident neutron producing two emitted neutrons] or transmuting reactions like (n,α) [one incident neutron producing a heavy residual nuclide with an atomic number Z reduced by two and an emitted light α particle], become important at higher PKA energies from where most damage will be created.

Fig. 1b shows the application of equation (4) for each neutron energy group (i.e. equation (4) without the sum over n) to the same $\{m_{kn}^{ij}\}$ vectors of recoil cross sections, and using the accepted standard threshold displacement energy E_d for Fe of 40 eV (see, for example, Table II in Ref. [22]). The figure shows the conversion from E_{PKA} to damage energy T_j, resulting in the shift to lower energy values on the x-axis, which can be clearly seen by comparing the upper limits of each curve to the curve of the same reaction channel in Fig. 1a. The calculation of dpa rates, which involves multiplication of cross sections by energy (see equation (4)) produces the change in profile of each curve compared to the PKA distributions: small damage energies (and hence PKA energies) produce relatively small dpa rates compared to higher energies. In contrast to the situation with the PKA distributions, for dpa the contributions from inelastic scattering and (n, 2n) on ^{56}Fe are as significant as those from the previously dominant elastic scattering.

Note that the results presented in this paper are for zero-time ($t = 0$) compositions of materials/nuclides before there has been any build-up of other, non-input nuclides due to transmutation reactions. As was shown previously [16], for the case of tungsten in a fusion environment, the growth of transmutation impurities during irradiation can cause a significant change in the PKA distributions (and hence possibly the dpa rate) as a function of time. This is beyond the scope of the present paper, but it is straightforward in SPECTRA-PKA to consider complex nuclide compositions, such as produced via transmutation and predicted by the time-evolution in an inventory simulation with FISPACT-II (see Ref. [16] for examples).

Of course, a real material, even if only a pure element, will usually be comprised of a number of different nuclides (including isotopes of the same element). For example, in pure Fe, there are four naturally occurring isotopes: ^{56}Fe (91.754 atomic %), ^{54}Fe (5.845%), ^{57}Fe (2.119%), and ^{58}Fe (0.282%). In such situations, the picture shown in Fig. 1 can become very complex and it is then difficult to discern anything useful from energy-dependent distributions of either PKAs or dpa rates. For dpa, applying equation (4) to obtain the total dpa rates for each reaction is more useful for understanding and interpretation (total and cumulative PKA distributions have been discussed elsewhere [7] as simplifications of the PKA picture).

The bar-plot in Fig. 2a, shows the SPECTRA-PKA results for the NRT-dpa rate contributions to various reaction channels in pure Fe under the fusion first wall spectrum (in Fig. 1a). The majority of the total dpa rate (9.2 NRT-dpa/year) comes from five main reactions on the primary ^{56}Fe isotope, with relatively small contributions from elastic and inelastic scattering on ^{54}Fe (0.4 dpa/year) and all other reactions on any target isotope (0.6 dpa/year). For the reactions on ^{56}Fe, elastic scattering dominates (3.8 dpa/year or 40.9% of the total, as shown in the plot in blue), followed by inelastic scattering (2.6 dpa/year or 28.1%) and the (n, 2n) channel (1.2 dpa/year or 12.9%).

The total dpa rate in Fig. 2a, obtained as the sum over all reaction

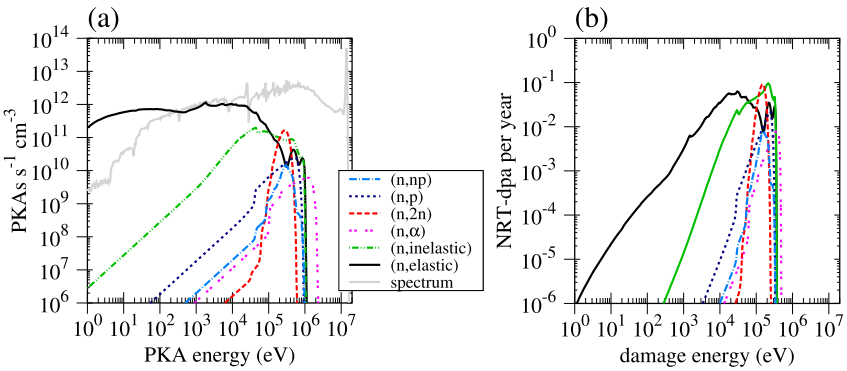

Fig. 1. (A) PKA spectra and (b) "dpa-spectra" for different reaction channels in pure ^{56}Fe irradiated in a typical neutron spectrum for the first wall of a demonstration fusion power plant (see Ref. [19] for details). The neutron irradiation spectrum is also shown in (a) with neutron flux in n cm^2 s^{-1} plotted against neutron energy in eV. See the main text for further details. (Colour online only).

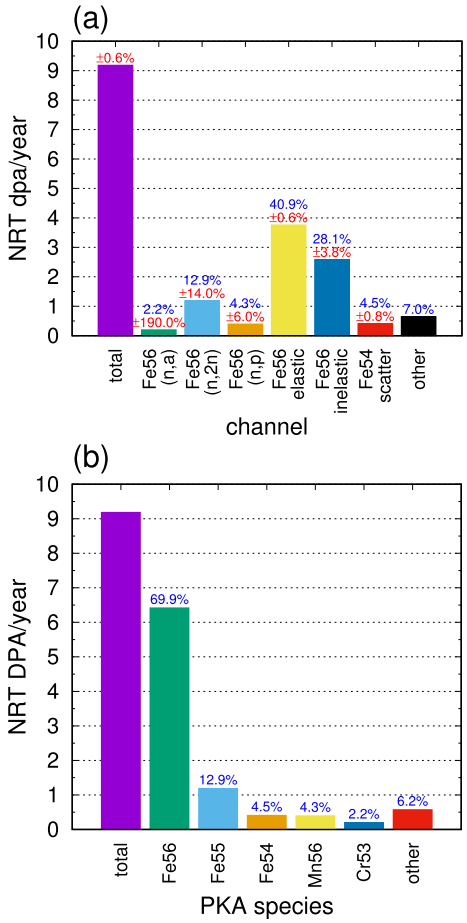

Fig. 2. (a) per-reaction-channel and (b) per-recoil-species dpa contributions to the total dpa rate in pure Fe irradiated in a typical neutron spectrum for the first wall of a demonstration fusion power plant (plotted in Fig. 1a). The values in blue above each bar are the % of the total dpa rate produced by that reaction channel or recoiling species. Additionally, in (a), values in red give the percentage uncertainty estimates derived from the covariances available for each reaction channel in the TENDL data used in the calculation – see the main text for more details. (Colour online only). (For interpretation of the references to colour in this figure legend, the reader is referred to the Web version of this article.)

channels and all target nuclides, agrees with equivalent dpa calculations performed using the standard application of equation (2) in FISPACT-II [9]. In turn, FISPACT-II has been shown to agree with other evaluations of integrated damage; for example, FISPACT-II predicts 0.042 total dpa in steel after 40 years in a typical PWR reactor pressure vessel (at quarter thickness with a 0.8 load factor) [23], in agreement with the 0.045±0.05 dpa reported in Ref. [24].

Fig. 2a also includes an estimate of the uncertainty associated with the dpa rate computed for each channel. The % uncertainties shown (as red text) above each bar in the plot are taken directly from the nuclear data uncertainties calculated by FISPACT-II for each reaction channel during folding with the fusion first wall neutron spectrum. There are exceptions for the total dpa uncertainty, which comes from the total cross section data channel (MT = 1 in ENDF-6 [25] format nomenclature) of ^{56}Fe, and the scatter uncertainty on ^{54}Fe, which again comes from the MT = 1 uncertainty (elastic and inelastic scattering make up more than 99.9% of the total cross section on ^{54}Fe in this case). Uncertainties are not presented in any other figures in this paper because those plots show the combined results for multiple reaction channels (e.g. the same reaction across multiple nuclides of the same element) and thus uncertainties are not straightforward to compute (or extract from elsewhere). Full inclusion and propagation of uncertainties, both for PKA spectra and dpa calculations, in SPECTRA-PKA is part of ongoing development of the code, and those given in Fig. 2a exemplify how this could be achieved.

Another summing approach is to consider the dpa contributions as a function of the recoiling (PKA) species that produces the damage. This is built-in to the analysis in SPECTRA-PKA and Fig. 2b displays the distribution of dpa rate contributions from different PKA species for the same Fe evaluation as in Fig. 2a. As would be expected, dpa from ^{56}Fe PKAs dominate – producing nearly 70% of the total dpa rate – because elastic and inelastic scattering on that nuclide, which is the majority of the target composition, also generate it as a PKA. ^{55}Fe nuclides, produced by (n, 2n) reactions on ^{56}Fe, are responsible for around 13% of the dpa and scattering on ^{54}Fe also makes a small contribution (as dpa from ^{54}Fe recoils). There are also contributions from ^{56}Mn and ^{53}Cr, i.e. damage from non-iron nuclides, produced via (n,p) and (n,α) reactions, respectively, on ^{56}Fe. It is worth highlighting here that the atomic number, excitation state, and decay properties of the PKA daughter are not presently accounted for in simulations (atomistic or otherwise) of radiation damage production and evolution; a situation that SPECTRA-PKA can help to address in the future with this separation of PKA and dpa rates by reaction channel (and daughter type). Note further, that SPECTRA-PKA includes the dpa from the recoiling protons (p) and ^{4}He nuclei (α) of these latter two reactions, but the resulting dpa rates are very small due to the large disparity in mass between atoms of the host iron lattice and the emitted p/α

particles.

Fig. 3 shows results for another pure element, W, under the same fusion spectrum shown in Fig. 1a. Once again the dpa results are separated by reaction type (Fig. 3a) and PKA species (Fig. 3b). However, differing from the Fe case above, tungsten has four major isotopes, ^{182}W, ^{183}W, ^{184}W, and ^{186}W, that all have similar concentrations in naturally occurring pure W (ranging from 14 to 30 atomic %). Thus, in Fig. 3a, the dpa contributions from different reaction channels are actually the sum over all W isotopes. Note that the threshold displacement energy E_d assumed for W in these calculations was 55 eV, which is a recent evaluation [26] based on experimental measurements of single atomic displacements [27], and not the historical 90 eV quoted elsewhere (e.g. in Ref. [22]).

In contrast to the scattering dominance seen in Fe, for W, Fig. 3a shows that neutron multiplication (n, 2n) reactions are responsible for almost as much of the predicted dpa damage dose as scattering (elastic and inelastic scattering have been summed together here) under this fusion neutron irradiation spectrum; 44.7% for (n, 2n) versus 54.1% for scattering out of the ~ 5 dpa/year total. There is also virtually no contribution from other reaction types, particular gas producing ones, such as (n,p) and (n,α), which is in agreement with calculations elsewhere, e.g. in Ref. [28], showing that gas production is relatively minor in W under fusion conditions compared to Fe. Note, however, that in W these gas-producing channels – particularly the (n,α) reactions – have positive Q-values, meaning that energy is released when they occur. Even in the latest TENDL [10] evaluations these non-threshold reactions may be underestimated below the unresolved resonance region [29], and so a different picture of their relative importance, for both gas production and dpa damage, may be predicted in the future.

The absence of significant contributions from reactions other than scattering and (n, 2n) results in negligible dpa from non-W PKA species in Fig. 3b, where there is a fairly even distribution of dpa rates among six different W nuclides. The highest contributions come from recoiling ^{182}W and ^{183}W nuclides because PKAs of these nuclides are produced via both neutron-scattering and neutron multiplication (on ^{183}W and ^{184}W, respectively).

Conversely, in Ni, there is a much greater contribution to the dpa from non-scattering, transmuting reactions – (n,p), (n,np) and (n,α) – due to the relatively high reaction cross sections of such reactions in this element, particularly at the 14 MeV peak of the fusion spectrum considered here (see, for example, [30,31]). Fig. 4a shows that more than 30% of the total dpa/year in pure Ni comes from

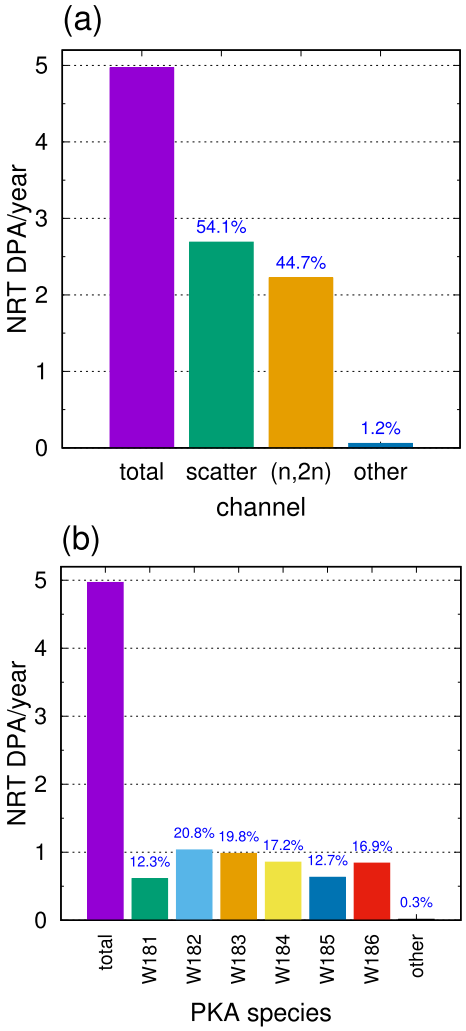

Fig. 3. (a) per-reaction-type and (b) per-recoil-species dpa contributions to the total dpa rate in pure W irradiated in a typical neutron spectrum for the first wall of a demonstration fusion power plant (plotted in Fig. 1a). The values above each bar are the % of the total dpa rate produced by that reaction type or recoiling species. (Colour online only).

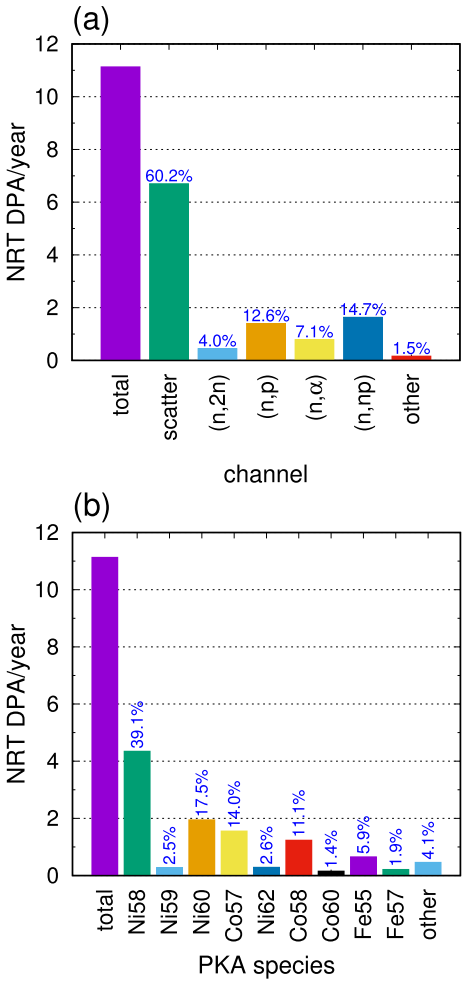

Fig. 4. (a) per-reaction-type and (b) per-recoil-species dpa contributions to the total dpa rate in pure Ni irradiated in a typical neutron spectrum for the first wall of a demonstration fusion power plant (plotted in Fig. 1a). The values above each bar are the % of the total dpa rate produced by that reaction type or recoiling species. The standard 40 eV threshold displacement energy E_d for pure nickel was assumed for these calculations [22]. (Colour online only).

such reactions in a first wall fusion environment, including 12.6% from (n,p), 7.1% from (n,α), and 14.7% from (n,np). Scattering is still dominant (more than 60% of the 11 dpa/year total), but other reactions, such as (n, 2n), are not significant contributors to the total. This results in a much greater variety of non-Ni recoil nuclides being responsible for significant amounts of the predicted dpa, including more than 20% of the total from Co PKAs (see Fig. 4b), which would result in different damage production and evolution.

3.1. Complex materials

One benefit of the SPECTRA-PKA approach for dpa calculation is that E_d is a user-defined variable and so can be chosen to best fit the material composition being considered. This differs from the approach taken for mixed compositions in FISPACT-II [9], where the threshold displacement energy varies with the parent nuclide – i.e. in a material containing, for example, Fe and W, the dpa contribution from nuclear reaction on the Fe nuclides would apply the Fe 40 eV standard E_d value, while for that calculated for reactions with the W nuclides, the W E_d value of 55 eV would be applied. While this might be a reasonable approximation in some cases, in a lattice dominated by nuclides of one particular element it could be more appropriate to use the threshold displacement energy of that element. Similarly, in an evenly mixed material, using an average E_d value might be suitable – a facility afforded by the SPECTRA-PKA methodology.

Furthermore, there is no limit to the complexity of the material (i.e. number of different nuclides) that may be considered in a SPECTRA-PKA calculation (subject to computational memory limits), and so it is straightforward to analyze both the PKA distributions and dpa/year breakdown for complex alloy compositions. 316 stainless steel (SS316) is a commonly used steel in nuclear applications and is being considered as the primary structural steel for the vacuum vessel of a future demonstration power plant (although not necessarily for in-vessel components due to its poor activation characteristics) [19]. The contributions to the total 9.5 dpa/year in the starting composition (as given in Ref. [19]) of SS316 under fusion first wall conditions are shown in Fig. 5.

Here the contributions are grouped according to the element type of the recoiling PKA species – there are too many different channels and recoil nuclides to group the contributions according to those. A value of 40 eV has been assumed for E_d, which is the literature value for the dominant Fe, Cr, and Ni elements in the matrix. Analysis of the impact of allowing E_d to vary according to the recoil element is beyond the scope of this paper, but is unlikely to have significant impact here due to the dominance of Fe, Cr, and Ni and their equal E_d values. As would be expected, recoiling nuclides of Fe, Cr, and Ni, which make up 63.4, 19.2 and 11.8 atomic %, respectively, of the input composition, are the dominant contributions to the dpa/year – responsible for 55.6, 19.3 and 8.9%, respectively, of the total dpa. However, Co, which is only present in SS316 at the 500 appm level, nonetheless contributes almost 4% of the dpa because, as seen in Fig. 4b, it is produced in significant amounts as a recoiling element in Ni. Similarly, PKAs of vanadium contribute more than 1% of the dpa, despite not being present in SS316, due to their creation via (n,p) reactions on Cr.

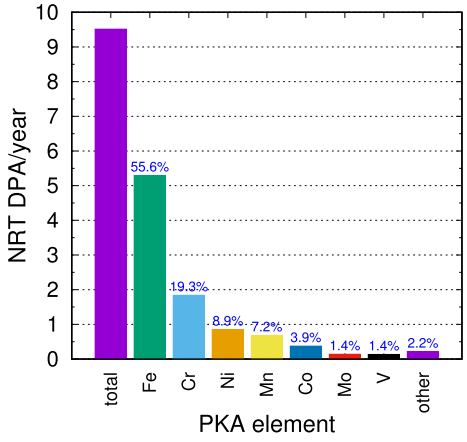

Fig. 5. Per-element-type dpa contributions to the total dpa rate in SS316 irradiated in a typical neutron spectrum for the first wall of a demonstration fusion power plant (plotted in Fig. 1a). The values above each bar are the % of the total dpa rate produced by that element's recoiling species. (Colour online only).

3.2. Fusion vs. fission

The authors have previously [28] compared the fusion and fission environments using FISPACT-II [9], in particular considering gas-to-dpa ratios for a wide range of different elements. With the new developments described here for SPECTRA-PKA, it is now instructive to consider the variation in contributions to dpa due to changing the irradiation environment. Fig. 6 shows reaction channel contributions to the total dpa/year in pure Fe and W under typical conditions at the high-flux reactor (HFR) at Petten in the

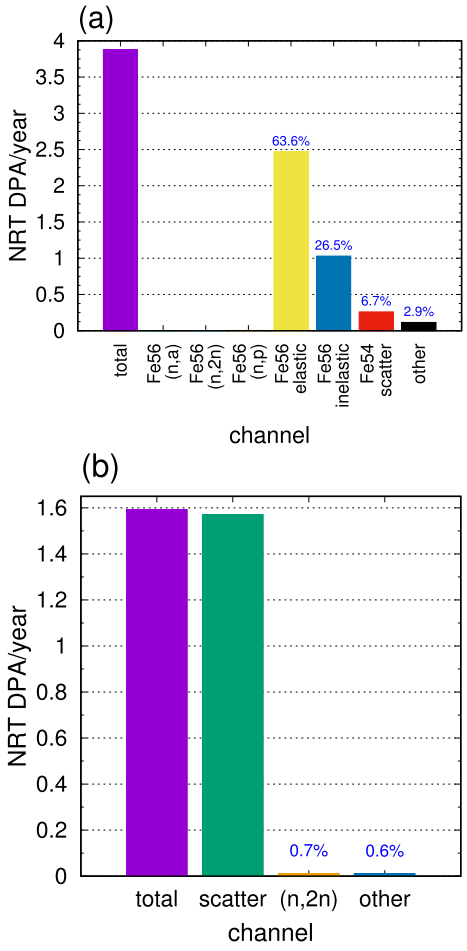

Fig. 6. Per-reaction-type dpa contributions to the total dpa rate in (a) pure Fe and (b) pure W irradiated in the neutron spectrum of the high-flux reactor (HFR) at NRG, Petten. In (b) the results for each reaction channel are the sum of that reaction on all W isotopes. The values above each bar are the % of the total dpa rate produced by that reaction type. (Colour online only).

Netherlands (further details of the spectrum used are given in Ref. [28]). This spectrum is significantly softer (has a greater proportion of low-energy or thermal neutrons) than the hard, fusion spectrum considered elsewhere in this paper. For both Fe (Fig. 6a) and W (Fig. 6b), and indeed for materials in general, this results in a greater importance of the scattering reaction channels because elastic scattering, in particular, has no threshold and is thus dominant below the thresholds of other reactions.

Note that HFR is, by design, a high flux reactor to promote the production of medical isotopes via transmutation. While this means that the absolute dpa rates presented here are higher than those expected in fission power reactors, the qualitative picture of contributions from specific reaction channels is the same (this has been confirmed via repeat calculations, not shown here, for a typical pressurized water reactor or PWR, whose spectrum is also discussed in Ref. [28]).

In contrast to the picture in fusion (Fig. 2a), for Fe under HFR conditions (Fig. 6a) the scattering channels make up almost 100% of the 3.9 dpa/year total (even the "other" in the figure is almost entirely scattering on the two remaining naturally occurring isotopes of Fe), while the contributions from the more complex (n, 2n), (n,p), and (n,α) reactions on ^{56}Fe, which contributed around 20% of the total dpa/year under fusion conditions, are entirely absent here. The situation is even more stark in W, where in HFR, (n, 2n) reactions produce less than 1% of the total (1.6 dpa/year) instead of nearly 50% of the total under fusion conditions (Fig. 3a), although in both cases recoiling W nuclides produce nearly 100% of the dpa.

These examples highlight how different the neutron environments in a fusion reactor will be compared to existing fission reactors (next generation, GEN-IV, fast fission systems will be more similar to fusion), and thus how challenging and damaging the different environment is for the materials and components that must withstand it.

4. Summary

This paper described an alternative approach to calculating displacement per atom (dpa) rates in materials. The recently developed SPECTRA-PKA code uses the same recoil cross sections that it has previously [7] used to evaluate the energy distributions of primary knock-on atoms (PKAs) in (neutron) irradiated materials, to instead apply the modified Kinchin-Pease or Norgett-Robinson-Torrens (NRT) formula (and associated Lindhard-Scharff-Schøtt energy partition functions) to calculate dpa on a per-reaction-channel basis.

The application of this new methodology to several important elements under neutron irradiation provides insight into the contribution to dpa from different reaction channels. Elastic and inelastic scattering channels are predictably dominant, due to their high cross sections at low neutron-energies, but in certain materials and under predicted fusion power plant conditions, more exotic nuclear reactions are responsible for a significant proportion of the predicted dpa rates. In W, for example, neutron multiplication (n, 2n) contributes almost 50% of the predicted dpa rate, while in Ni, gas-producing reactions (e.g. (n,p), (n,α)) contribute more than 30% to the dpa/year.

The contributions from different reaction channels can also vary significantly with the irradiation environment. Under typical light water reactor (LWR) fission conditions (i.e. HFR) it was found that scattering produces most of the damage, even in materials where other reactions were important under fusion conditions.

The contributions from different reaction channels can also vary significantly with the irradiation environment. Under typical fission conditions it was found that scattering produces most of the damage, even in materials where other reactions were important under fusion conditions.

The rigorous methodology described in this paper, and implemented in SPECTRA-PKA, provides scope for new and novel interpretation and understanding of nuclear reaction data, and the relative importance of different parts (channels) of that data to material degradation.

Acknowledgements

This work was funded by the RCUK Energy Programme [grant number EP/P012450/1]. To obtain further information on the data and models underlying this paper please contact PublicationsManager@ukaea.uk.

References

[1] M.J. Norgett, M.T. Robinson, I.M. Torrens, A proposed method of calculating displacement dose rates, Nucl. Eng. Des. 33 (1975) 50–54, https://doi.org/10.1016/0029-5493(75)90035-7.
[2] G.R. Odette, D.R. Doiron, Neutron-energy-dependent defect production cross sections for fission and fision applications, Nucl. Tech. 29 (1976) 346–368, https://doi.org/10.13182/NT76-A31600.
[3] M.R. Gilbert, S. Zheng, R. Kemp, L.W. Packer, S.L. Dudarev, J. -Ch. Sublet, Comparative assessment of material performance in demo fusion reactors, Fusion Sci. Technol. 66 (2014) 9–17, https://doi.org/10.13182/FST13-751.
[4] M.R. Gilbert, S.L. Dudarev, S. Zheng, L.W. Packer, J. -Ch. Sublet, An integrated model for materials in a fusion power plant: transmutation, gas production, and helium embrittlement under neutron irradiation, Nucl. Fusion 52 (2012), 083019, https://doi.org/10.1088/0029-5515/52/8/083019.
[5] Y. Dai, G.R. Odette, T. Yamamoto, The effects of helium in irradiated structural alloys, in: R. Konings (Ed.), Comprehensive Nuclear Materials, Elsevier, Oxford, 2012, pp. 141–193, https://doi.org/10.1016/B978-0-08-056033-5.00006-9.
[6] G.H. Kinchin, R.S. Pease, The displacement of atoms in solids by radiation, Rep. Prog. Phys. 18 (1) (1955) 1, https://doi.org/10.1088/0034-4885/18/1/301.
[7] M.R. Gilbert, J. Marian, J. -Ch. Sublet, Energy spectra of primary knock-on atoms under neutron irradiation, J. Nucl. Mater. 467 (2015) 121–134, https://doi.org/10.1016/j.jnucmat.2015.09.023.
[8] M.R. Gilbert, SPECTRA-PKA, SPECTRA-PKA is available as a utility within FISPACT-II, and now also available to download from github at. https://github.com/fispact/SPECTRA-PKA, 2018.
[9] J.-Ch. Sublet, J.W. Eastwood, J.G. Morgan, M.R. Gilbert, M. Fleming, W. Arter, FISPACT-II: an advanced simulation system for activation, transmutation and material modelling, Nucl. Data Sheets 139 (2017) 77–137, https://doi.org/10.1016/j.nds.2017.01.002.
[10] A.J. Koning, D. Rochman, Modern nuclear data evaluation with the TALYS code system, Nucl. Data Sheets 113 (12) (2012) 2841–2934, https://doi.org/10.1016/j.nds.2012.11.002 special Issue on Nuclear Reaction Data.
[11] D. Rochman, A.J. Koning, J.-Ch. Sublet, M. Fleming, E. Bauge, S. Hilaire, P. Romain, B. Morillon, H. Duarte, S. Goriely, S. van der Marck, H. Sjöstrand, S. Pomp, N. Dzysiuk, O. Cabellos, H. Ferroukhi, A. Vasiliev, The TENDL library: hope, reality and future, EPJ Web Conf. 146 (2017) 02006, https://doi.org/10.1051/epjconf/201714602006.
[12] A. J. Koning, D. Rochman, J.-Ch Sublet, TENDL-2017, release Date: December 30, 2017. Available from: https://tendl.web.psi.ch/tendl2017/tendl2017.html.
[13] R. E. MacFarlane, D. W. Muir, R. M. Boicourt, A. C. Kahler, The NJOY nuclear data processing system – LA-UR-12-27079, http://t2.lanl.gov/nis/publications/NJOY2012.pdf (Version 2012-032).
[14] J. Lindhard, M. Scharff, H.E. Schiøtt, Range concepts and heavy ion ranges (notes on atomic collisions, II), Mat. Fys. Medd. Dan. Vid. Selsk 33 (14) (1963) l–42. https://www.osti.gov/scitech/biblio/4153115.
[15] J. Lindhard, V. Nielsen, M. Scharff, P.V. Thomsen, Integral equations governing radiation effects (notes on atomic collisions, III), Mat. Fys. Medd. Dan. Vid. Selsk 33 (10) (1963) l–42.
[16] M.R. Gilbert, J.-Ch. Sublet, PKA distributions: contributions from transmutation products and from radioactive decay, Nucl. Mater. Energy 9 (2016) 576–580, https://doi.org/10.1016/j.nme.2016.02.006.
[17] M.T. Robinson, Basic physics of radiation damage production, J. Nucl. Mater. 216 (1994) 1–28, https://doi.org/10.1016/0022-3115(94)90003-5.
[18] M.T. Robinson, The energy dependence of neutron radiation damage in solids, in: J.L. Hall, J.H.C. Maples (Eds.), Nuclear Fusion Reactors, British Nuclear Energy Society, London, 1970, pp. 364–378, https://doi.org/10.1680/nfr.44661.0025.
[19] M.R. Gilbert, T. Eade, C. Bachmann, U. Fischer, N.P. Taylor, Activation, decay heat, and waste classification studies of the European DEMO concept, Nucl. Fusion 57 (2017), 046015, https://doi.org/10.1088/1741-4326/aa5bd7.
[20] L. Lunéville, D. Simeone, C. Jouanne, Calculation of radiation damage induced by neutrons in compound materials, J. Nucl. Mater. 353 (1) (2006) 89–100, https://doi.org/10.1016/j.jnucmat.2006.03.006.
[21] A. J. Koning, D. Rochman, J. Kopecky, J.-Ch Sublet, M. Fleming, E. Bauge, S. Hilaire, P. Romain, B. Morillon, H. Duarte, S. van der Marck, S. Pomp, H.

Sjostrand, R. Forrest, H. Henriksson, O. Cabellos, S. Goriely, J. Leppanen, H. Leeb, A. Plompen, R. Mills, TENDL-2015, release Date: January 18, 2016. Available from: https://tendl.web.psi.ch/tendl2015/tendl2015.html.

[22] R.E. MacFarlane, A.C. Kahler, Methods for processing ENDF/B-VII with NJOY, Nucl. Data Sheets 111 (2010) 2739–2890, https://doi.org/10.1016/j.nds.2010.11.001.

[23] J.-Ch. Sublet, M. R. Gilbert, S. L. Dudarev, "Radiation damage: beyond dpa: from nuclear data to materials sciences", presented at the first research coordination meeting on the IAEA coordinated research project (CRP) on "Primary Damage Cross Sections" (Vienna, Austria, 4–8 November, 2013). URL https://www-nds.iaea.org/CRPdpa/RCM1_Presentations/Sublet_Beyond-dpa-IAEA.pdf.

[24] G.R. Odette, G.E. Lucas, Embrittlement of nuclear reactor pressure vessels, JOM (Journal of The Minerals, Metals & Materials Society) 53 (2001) 18–22, https://doi.org/10.1007/s11837-001-0081-0.

[25] M. Herman, A. Trkov, D.A. Brown (Eds.), ENDF-6 Formats Manual, Data Formats and Procedures for the Evaluated Nuclear Data File ENDF/B-VI and ENDF/B-vii, Vol. BNL-90365–92009 Rev. 2, Brookhaven National Laboratory, 2012. https://www-nds.iaea.org/public/endf/endf-manual.pdf.

[26] D.R. Mason, X. Yi, M.A. Kirk, S.L. Dudarev, Elastic trapping of dislocation loops in cascades in ion-irradiated tungsten foils, J. Phys. Condens. Matter 26 (37) (2014) 375701, https://doi.org/10.1088/0953-8984/26/37/375701.

[27] F. Maury, M. Biget, P. Vajda, A. Lucasson, P. Lucasson, Frenkel pair creation and stage I recovery in W crystals irradiated near threshold, Radiat. Eff. 38 (1–2) (1978) 53–65, https://doi.org/10.1080/00337577808233209.

[28] M.R. Gilbert, J.-Ch. Sublet, Scoping of material response under DEMO neutron irradiation: comparison with fission and influence of nuclear library selection, Fusion Eng. Des. 125 (2017) 299–306, https://doi.org/10.1016/j.fusengdes.2017.06.016.

[29] M.R. Gilbert, J.-Ch. Sublet, S.L. Dudarev, Spatial heterogeneity of tungsten transmutation in a fusion device, Nucl. Fusion 57 (2017), 044002, https://doi.org/10.1088/1741-4326/aa5e2e.

[30] M. Griffiths, L. Walters, L. Greenwood, F. Garner, Accelerated materials evaluation for nuclear applications, J. Nucl. Mater. 488 (2017) 46–62, https://doi.org/10.1016/j.jnucmat.2017.02.039.

[31] M. Fleming, J.-Ch. Sublet, J. Kopecky, Integro-differential Verification and Validation, FISPACT-II & TENDL-2014 nuclear data libraries, Tech. Rep. (2015). CCFE-R(15)27, CCFE, available from: www.fispact.ukaea.uk.